Journal of Materials Chemistry B

Accepted Manuscript

ROYAL SOCIETY OF CHEMISTRY

www.rsc.org/materialsB

Journal Name

RSCPublishing

ARTICLE

Multicavity halloysite-amphiphilic cyclodextrin hybrids for co-delivery of natural drugs into thyroid cancer cells

Cite this: DOI: 10.1039/xoxxoooooox

Received ooth January 2012,
Accepted ooth January 2012

DOI: 10.1039/xoxxoooooox

www.rsc.org/

M. Massaro,[a] S. Piana,[a] C. G. Colletti,[a] R. Noto,[a] S. Riela,[*a] C. Baiamonte,[b] C. Giordano,[b] G. Pizzolanti,[b] G. Cavallaro,[c] S. Milioto,[c] and G. Lazzara.[*c]

Multicavity halloysite nanotube materials were employed as simultaneous carrier for two different natural drugs, silibinin and quercetin, at 6.1% and 2.2% drug loadings, respectively. The materials were obtained by grafting functionalized amphiphilic cyclodextrin onto HNT external surface. The new materials were characterized by FT-IR spectroscopy, SEM, thermogravimetry and turbidimetry, dynamic light scattering and ζ-potential techniques. The interaction of the two molecules with the carrier was studied by HPLC measurements and fluorescence spectroscopy, respectively. Release of the drugs from HNT-amphiphilic cyclodextrin, at two different pH values was also investigated by means UV-vis spectroscopy. Biological assays showed that the new complex exhibits an anti-proliferative activity against the human anaplastic thyroid cancer cell lines 8505C. Furthermore, fluorescence microscopy was used to evaluate whether the carrier was be uptaken into 8505C thyroid cancer cell lines. The successful results revealed that the synthesized multicavity system is a material of suitable size to transport drugs into living cells.

Introduction

In recent years, there is an increasing interest in both life and materials science to use nanocontainers as carriers for the encapsulation and delivery of drug molecules.
Halloysite nanotubes (HNTs) is a biocompatible aluminosilicate clay, with a hollow tubular structure consisting of silica on the outer surface and alumina at the innermost surface.[1] HNTs and functionalized-HNTs (f-HNTs) are capable of entrapping a variety of active agents within the inner lumen as well as at the external surface, followed by their retention and slow release.[2] Due to their appealing characteristics, various exciting applications has been proposed for these nanomaterials. For instance, biomedical applications of HNTs include their use as gene delivery systems, cancer cell isolation, stem cell isolation, ultrasound contrast agents, bone implants, teeth fillers, cosmetics and controlled drug delivery.[3-8]
Cyclodextrins (CDs) are very promising materials in several fields. It is known that these macrocyclic compounds form inclusion complexes with small- and medium-sized organic molecules and the complexation reactions that are involved are highly important in drug delivery systems.[9] Furthermore, it was demonstrated that the use of amphiphilic cyclodextrins in drug delivery applications allows to increase the range of potential drugs that can be encapsulated in the CD cavity.[10]
Recently we reported the first example of a new drug delivery system based on HNT covalently linked to modified-cyclodextrin units employed as carrier for polyphenolic compounds like curcumin.[11]
Polyphenolic compounds, like flavonoids, that are ubiquitously distributed in plant have attracted considerable interest for their wide variety biochemical and pharmacological properties.[12,13] Unfortunately, their concentration in the blood circulation is likely to be low because they are sparingly soluble in water and chemically unstable in physiological medium.[14-16]
In order to protect these bioactive compounds against degradation factors and to enhance the bioavailability, various encapsulation and complexation methods are used.
In the present paper we describe the synthesis and the characterization of a novel hybrid based on HNT covalently linked to amphiphilic-cyclodextrin units. The advantages of multifunctional nanocarriers with the presence of two cavities offers the remarkable possibility for a simultaneous encapsulation of one or more drug molecules with different physico-chemical properties, followed by a different path release in agreement of the cavity that interacts with the drugs. Therefore, in order to employ the new system as a drug carrier we also studied its simultaneous interaction with two molecules, namely quercetin and silibinin, that possess different size and shape (Figure 1).

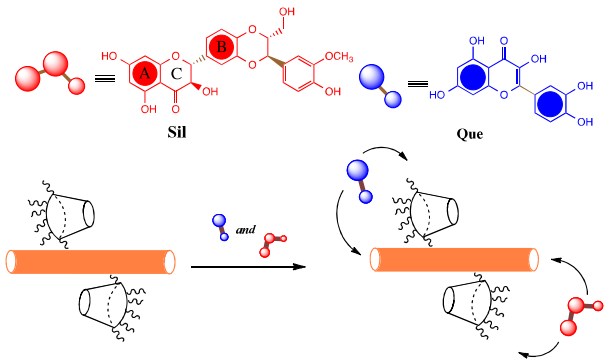

Figure 1. Halloysite nanotubes-amphiphilic cyclodextrin drug carrier.

Indeed, co-delivery has attracted more and more attention because it is known that compared to conventional single-agent treatment, multi-agent therapy can promote synergism of different drugs, increase therapeutic target selectivity, and overcome drug resistance through distinct mechanisms of action.[17]

Results and discussion

Pristine halloysite was transformed as described into f-HNT-CD **1**,[10] and we used this material as scaffold for the covalent linkage of alkyl thiols **2a-d** by thiol-ene reaction between vinyl groups on CDs and -SH groups on thiols (Scheme 1).

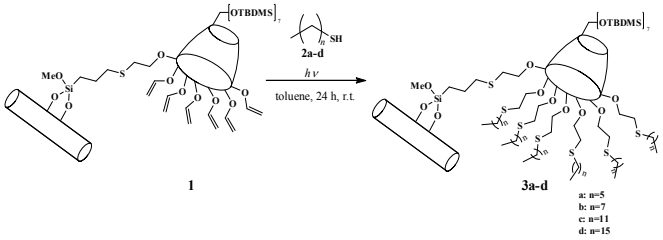

Scheme 1. Schematic representation for the linkage of alkyl thiols on compound **1**.

The reaction of **1** with alkyl thiols **2** was carried out by irradiation with UV light, from Hg lamp, using toluene as solvent, in a quartz vials at room temperature under argon atmosphere. After 24 h the compounds **3a-d** were obtained and analysed by TGA in order to evaluate the percentage of the loading, that was in the range among 0.6-2.9%.
It is interesting to note that, with increasing of alkyl chain length of thiol (from **3a** to **3d**), we obtained materials with lower percent loading (2.9 and 0.9%, respectively), as a consequence of enhanced steric hindrance on HNT surface.
The grafting degrees provided an idea in terms of average positions substituted in the CD, namely it comes out that in **3a** and **3b** the allyl groups have been fully substituted while **3c** and **3d** have an average of two substituted allyl groups.
The new materials were characterized by FT-IR spectroscopy, TGA and SEM measurements.
FT-IR investigation on **3a-d** shows that the vibrational bands of HNTs remain unaltered after the reactions. The frequency and assignments of each vibrational mode are based on previous reports on halloysite.[18]
Compared to **1** compounds **3a-d** exhibit an increase in the intensity of vibration bands for C-H stretching of methylene groups around 2960 cm^{-1} and 2865 cm^{-1} (see ESI).

The samples **3a-d** were investigated by means of TGA to determine the grafted amount of organic moieties. From a comparison with the thermogram for **1**, a further degradation and volatilization is observed accounting for the additional organic fraction. The grafting degrees were determined by comparing the residual masses at 900 °C of each **3a-d** and **1**. The obtained values are rather similar and range between 0.6 and 2.9 wt%.
Direct observation of the surface morphology of **3a-d** was accomplished by SEM. In all cases the tubular shape of the nanoclay is not lost after grafting. Moreover, the lumen of the functionalized nanotubes appears empty, in agreement with the expected grafting at the external surface (Figure 2).

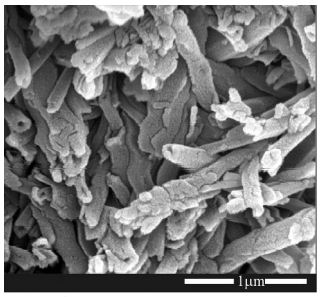

Figure 2. SEM images of **3a**.

Studies of the dispersions in aqueous medium

Turbidimetric analysis was performed to highlight the influence of functionalization on the dispersion stability of HNT in aqueous media, which might be crucial for its application as a drug delivery system. Dispersions of **3a-c** showed a lower stability in water than **1**, according to the more hydrophobic surface functionalization in **3a-b** as compared to **1** (Figure 3).
On the contrary, dispersions of **3d** showed higher aqueous stability (Figure 3) than **3a-b** and, surprisingly, even than **1**.

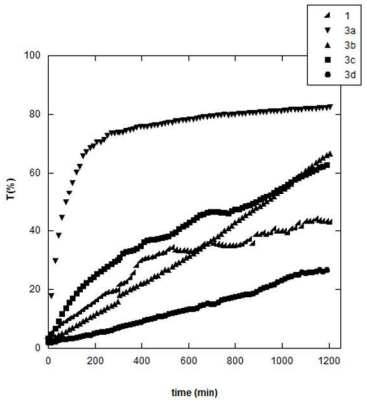

Figure 3. Optical transmittance as a function of time for **1** and **3a-d** dispersions in water. The concentration is 0.1 wt% in all cases.

It is known[19] that the presence of polymer and/or surfactant at the nanoparticle surface may, generally, cause two different effects: (i) hydrophobic interactions, that involve aggregation of material; (ii) steric repulsion or osmotic effect that involve an increasing in repulsive interactions between nanoparticles and this, generates stabilization of the dispersions.
The stability of the dispersions of compounds **3a-c** is controlled by hydrophobic interactions, while for **3d** a steric stabilization may occur.

The diffusion coefficient of the nanoparticles in the solvent confirmed the results obtained by turbidimetric analysis. The diffusion coefficients of **3a-d** obtained by DLS experiments are collected in Table 1:

Table 1. Diffusion coefficients for modified HNTs.

Entry	Sample	D (10^{-13} m^2 s^{-1})
1	**3a**	5.57
2	**3b**	5.93
3	**3c**	9.53
4	**3d**	9.01

By comparing these results with the diffusion coefficient of **1** (11×10^{-13} m^2s^{-1}) and HNT in water (9.4×10^{-13} m^2s^{-1})[20] it appears that **3a-b** form aggregates while **3c-d** show no aggregation.
With the aim at evidencing possible changes in the nanoparticle-nanoparticle electrostatic interactions, the ζ-potential in water was measured. All samples **3a-d** showed negative ζ-potential values (ca. -20 mV) close to that of HNT (-19.5 mV). Therefore the electrostatic nanoparticle-nanoparticle repulsions are not altered by the surface functionalization, confirming that the aggregation of **3a-b** compounds is driven by van der Waals interaction and hydrophobic effects.

Interaction with silibinin and quercetin

With the aim to combine two or more drugs with synergistic therapeutic effect we verified the binding abilities of one of our new systems (**3a**) for two flavonoids, namely, silibinin (Sil) and quercetin (Que), chosen for their different affinity for the two cavities of the nanomaterial. We choose for the subsequent studies **3a** compound in order to overcome problems of native CD that limit their application in pharmaceutical fields, for example to (i) enhance the interaction of CD with biological membranes and (ii) modify or enhance interaction of CD with hydrophobic drugs.[21] It should be noted that **3a** has the highest loading (2.9 %) of amphiphilic cyclodextrin.
Experimental investigations performed by means of UV-vis and HPLC highlighted that silibinin did not interact with cyclodextrin cavity, by the contrast, it was encapsulated into pristine HNT lumen as found by UV-vis spectroscopy and TGA (see ESI).
It is reported that native βCD is efficient in including quercetin.[22] In order to verify that the CD modification does not hinder the quercetin inclusion, supramolecular interactions with amphiphilic CD (having the same substitution pattern of **3a**) has been studied. The formation of 1:2 quercetin/amph-CD complexes has been demonstrated by isothermal titration calorimetry (ITC) and UV-vis spectroscopy. The ITC data provided the equilibrium constant and enthalpy change for the quercetin/amph-CD inclusion complex formation by assuming the equilibria:

$$CD + Que \xrightleftharpoons{K_1} CD - Que$$

$$CD - Que + CD \xrightleftharpoons{K_2} CD - Que - CD$$

and the procedure reported elsewhere.[23]
It was found $\beta = K_1 \times K_2 = (6.3\pm0.3)\times10^5$ M^{-2} and ΔH_{ic}=-7.1 ± 0.3 kJ mol^{-1}, according to UV-vis results ($\beta = (9\pm2)\times10^5$ M^{-2}) (see ESI for details).
Furthermore fluorescence titration showed that this molecule also interacts with pristine HNT (see ESI). Recently, we have demonstrated that in the presence of HNT-cyclodextrin hybrid, curcumin, a biological molecule with similar structure of quercetin, interacts preferentially with cyclodextrin cavity.[11]
On the ground of these evidences we studied the interaction of **3a** with silibinin and quercetin by HPLC and fluorescence spectroscopy.
Reverse-phase HPLC equipped with Diode-Array/UV detector offers the remarkable advantage to record in real time the UV–vis spectrum of the chromatographic eluate (in the range 200–600 nm), and therefore it allows the simultaneous monitoring of different species/analytes.
According to previous reports,[24] pure silibinin showed two peaks in the HPLC chromatogram, corresponding to the diasteroisomers silibinin A and B, with retention times (rt) of 2.67 and 3.53 minutes respectively (eluent MeOH/H_2O 90:10 v/v, flow 1 mL min^{-1}). The most abundant component displayed two bands in the UV spectrum, the first one at 280 nm and the second one, less intense, at 320 nm ca.
Pure quercetin showed one peak in the chromatogram at rt of 3.38 min and it shows an UV spectrum with two bands at 250 and 370 nm.
No peaks were observed in the chromatogram related to **3a**, because this material shows no UV absorption.
Titration of fixed concentrations of silibinin and quercetin with **3a** (0-1.8 mg/mL) gave chromatograms (eluent MeOH/H_2O 90:10 v/v, flow 1 mL min^{-1}) which illustrated a no resolved broad peak at rt range between 3.00 and 3.50 min, and presented a UV spectrum showing the same absorption maxima of silibinin. However, with increasing amount of **3a** the UV spectrum displays a drastic change in intensity of signal at 320 nm (Figure 4).

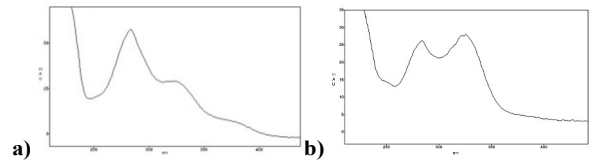

Figure 4. UV-vis spectra of a) silibinin and b) **3a**/silibinin complex.

It is known that dihydroflavonols show two major absorption bands: band I (300–400 nm) and band II (240–280 nm).[25] Band I originates due to light absorption of the A + C rings and corresponds to a π-π* transition; band II is due to the absorption of the B ring.
Therefore, because in our systems we have hypothesized that silibinin interacts with **3a** lumen, the different UV electronic absorption behaviour may be attributed to specific Sil-**3a** interactions in the form of hydrogen bonds and/or hydrophobic effect that involve phenolic OH groups of A rings. Similar results were obtained by Angelico et al. for encapsulation of silibinin into liposomes.[26]
Being that silibinin in aqueous medium does not show emission, the interaction of quercetin and **3a**, on the contrary, was studied by means of fluorescence spectroscopy.
The trend of fluorescence intensity of quercetin (1×10^{-4} M), recorded at 540 nm, with increasing amount of **3a** (0-1.5 mg/mL) is reported in Figure 5. This trend, related to the surnatant of the dispersions, is close to that obtained in the presence of crude amph-CD. Based on this finding and on the strong interaction evidenced by ITC and UV-vis between Que and amph-CD one may hypothesize that quercetin interacts preferentially with the cyclodextrin cavity (Figure 5). Similarly,

curcumin, an hydrophobic drug, was selectively incapsulated into the CD instead of the hydrophilic HNT cavity.[11]

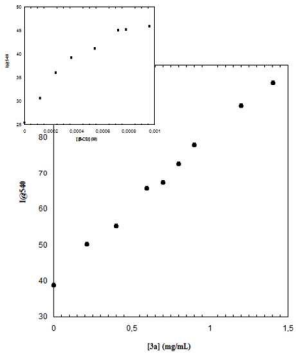

Figure 5. Trend of the fluorescence intensity of quercetin, recorded at 540 nm, as a function of **3a** concentration (0-1.8 mg/mL) in the presence of fixed amount of silibinin (1×10^{-4} M); the inset shows the fluorescence intensity of quercetin in the presence of increasing amount of β-CD.

Loading silibinin in the **3a** was carried out on vacuum cycling of a **3a** suspension in a saturated silibinin solution. This cycle was repeated several times in order to obtain the highest loading efficiency. After loading, the **3a**/Sil complex was washed in order to remove the free silibinin. **3a**/Sil was suspended again in water and then, to this dispersion a saturated solution of quercetin was added. Subsequent investigations were conducted on the dry solid filtered from dispersion, washed with water and dried overnight at 60 °C.
The composite solids **3a**/Sil and **3a**/Sil/Que were characterized by TGA (Figure 6). The thermoanalytical curves clearly show the successful loading of the drugs at each step. Given that both silibilin and quercetin degraded with a null residual at 900 °C, we calculated that compound **3a** is able to incorporate 6.1 % of silibilin and 2.2 % of quercetin. These results prove that the modified HNTs with a double cavity are efficient as nanocontainer for co-delivery of two biological active molecules.

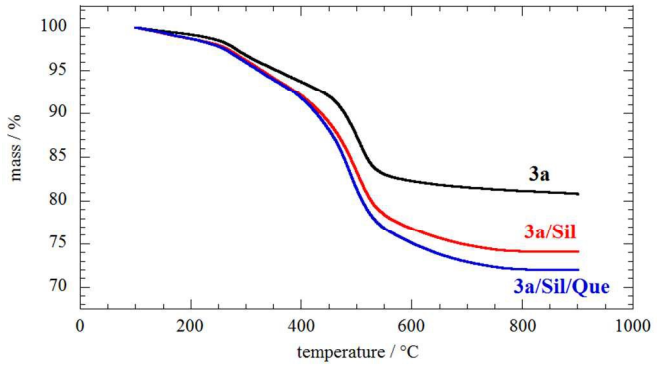

Figure 6. Thermoanalytical curves for **3a** before and after drugs loading.

Kinetic Release

In Figure 7 extended release profile of silibinin and quercetin from **3a**, in two different pH solution was elucidated.
The release of silibinin at pH 1 from compound **3a** reaches a plateau after 400 min, an initial burst is observed within 200 min followed by a prolonged release.

Release profile obtained for quercetin showed a similar behavior than silibinin, but in this case a very low amount of molecule was released from the system (Figura 7a). These results could be explained as follows. In acidic solution both **3a** and silibinin are positively charged; therefore, electrostatic repulsions may also accelerate the release of drug from **3a**. In the case of quercetin it was reported that the retention efficiency of Que on β-CD is depending on the pH, in particular it was larger in acidic solution than in neutral and basic medium.[27] Therefore, the small amount of quercetin released from **3a** at pH 1 could be explained on the basis of strong interaction of the molecules and CD cavity in acidic medium.

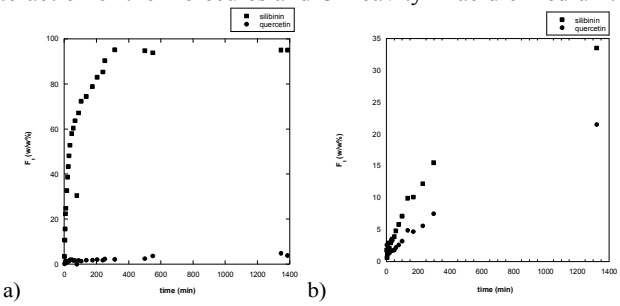

Figure 7. Amount of silibinin and quercetin released from **3a** in a) 0.1 M HCl solution; b) pH 7.4 phosphate buffer.

In physiological medium we observed that both molecules were released from the system; also in this case, quercetin was released in a smaller amount than silibinin. The different release in a neutral medium could be explained taking into account that flavonoids are in their neutral form in a pH range between 4 and 6; therefore at physiological pH they could be partially dissociated and so more soluble in aqueous medium.
To better understand the release behaviour of silibinin and quercetin in different pH situation, the *in vitro* release data were fitted to various model to analyse the kinetics and the release mechanism of both molecules. The experimental data were analysed using zero-order and first order equation, double exponential model (DEM) and the Power law, to elucidate the release kinetics of silibinin at pH 1 and 7.4 and of quercetin at pH 7.4. It was found that the release mode of silibinin in acidic solution follows the double exponential model. According to the literature,[28] the DEM describes a mechanism consisting of two parallel reactions involving two spectroscopically distinguishable species. In our particular case we observed the release of silibinin and the simultaneous, even if very low, release of quercetin (k = 0.007 ± 0.001 min^{-1} and k' = 0.064 ± 0.006 min^{-1}).
In physiological medium release mode of silibinin and quercetin follows, in both cases, the first-order kinetics (k = 0.0017 ± 0.0001 min^{-1} and 0.0007 ± 0.0001 min^{-1}, for silibinin and quercetin, respectively).
Desorption of silibinin and quercetin from **3a** can be described as the desorption of the molecules encapsulated into the HNT lumen and into β-CD cavity, respectively.

In *vitro* citotoxicity assay

We have tested the potential anti-proliferative in *vitro* activity of the **3a**/Sil/Que complex on an anaplastic thyroid cancer cell line: 8505C by means MTS tests.
The survival rates of the tumor cells incubated with **3a** at each concentration were found in the range of 96-100%, indicating they have no effect on cell viability of the tumor cell lines under the concentration conditions investigated. Free quercetin

and silibinin have no effect on cell viability, probably due to their rapid metabolism, systemic elimination and insolubility in physiological medium.
On the contrary, the cell line showed dose dependent cytotoxic profile when exposed at the treatment of **3a**/Sil/Que (see Figure 8).
In particular, the concentration of **3a**/Sil/Que which caused 50% inhibition of cell growth was 27.6 μM ± 6.1 Compared to the free drugs, the HNT nanoparticles significantly improved the cellular cytotoxicity and exhibited the obviously synergistic effect by the co-delivery of two different anticancer drugs silibinin and quercetin.

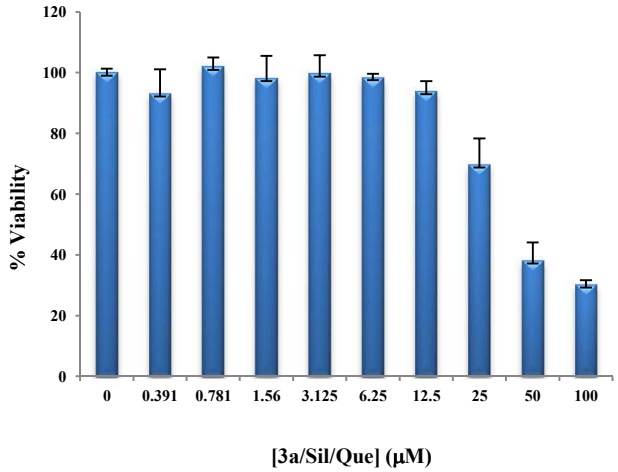

Figure 8. MTS test for cell viability of 8505C cells cultured for 72 h in presence of **3a**/Sil/Que.

Cellular uptake of drug into 3a

To the light of a potential application of **3a**/Sil/Que as novel therapeutic treatment, several tests have been carried out in *vitro* to evaluate their uptake and localization into 8505C thyroid cancer cell lines. Indeed, for internalization of nanoparticles by tumor cells it is essential to liberate therapeutic agents into cytosol where most therapeutic agents accumulate and take effect.
To this purpose, we analyzed, by means of fluorescence microscopy, the interaction between cells and the carrier.
Fluorescence microscopy data revealed that **3a** showed a high propensity to cross cell membranes resulting in a massive cell uptake, as highlighted by the fluorescence emission localized in the cytoplasm. In particular, halloysite nanoparticles penetrate into the cells and concentrate around cell nucleus from the observation of the silibinin fluorescent signal (green) within cells (Figure 9). The results suggested that the **3a**/Sil/Que complexes could effectively transport into living cells.

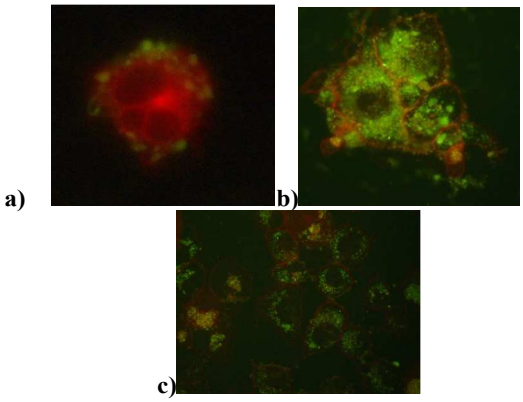

Figure 9. Fluorescence microscope images of the **3a** uptake by 8505C. 8505C cell membrane (red) with co-localised **3a** (green) outside nuclei at a) 1 h and b-c) 24 h.

Experimental section

All needed reagents were used as purchased (Aldrich), without further purification.
Cyclodextrin functionalized HNTs were prepared according to previous report.[11]
Heptakis-6-(tert-butyldimethylsilyl)-2-propaneoxy-2-hexanethio-□-cyclodextrin was synthesized as described below.
The chromatographic measurements were performed using a Shimadzu Class VP (Shimadzu, Japan) which consist of a pump (LC-10AD VP Shimadzu), an injection valve equipped with a 20 μL injection loop, an UV-vis Diode-Array (SPD-M10A VP) and an acquisition data software Class-VP. After optimization of chromatographic conditions, separation was carried out on C_{18} column (Discovery Supelco, 25 cm × 4.6 mm, 5 μm). The mobile phase consisted of methanol/water 90:10 v/v, at room temperature, flow 1 mL/min.
AESEM FEI QUANTA 200F microscope apparatus was used to study the morphology of the functionalized HNTs. Before each experiment, the sample was coated with gold under argon by means of an Edwards Sputter Coater S150A, in order to avoid charging under electron beam.
Thermogravimetric analyses were performed on a Q5000 IR apparatus (TA Instruments) under a nitrogen flow of 25 $cm^3 \cdot min^{-1}$ for the sample and 10 $cm^3 \cdot min^{-1}$ for the balance. The weight of each sample was ca. 10 mg. Measurements were carried out by heating the sample from rt up to 900 °C at a rate of 10 $°C \cdot min^{-1}$.
IR spectra (KBr) were recorded with an Agilent Technologies Cary 630 FT-IR spectrometer. Specimens for measurements were prepared by mixing 5 mg of the sample powder with 100 mg of KBr.
DLS measurements were performed at 22.0 ± 0.1 °C in a sealed cylindrical scattering cell at a scattering angle of 90°, by means of a Brookhaven Instrument apparatus composed of an BI-9000AT correlator and a He-Ne laser (75 mW) at a wavelength (λ) of 632.8 nm. The solvent was filtered through a 0.45 μm pore size Millipore filter with. For all systems, the field-time autocorrelation functions were well described by a mono-exponential decay function, which provides the decay rate (Γ) of the single diffusive mode. For the translational motion, the collective diffusion coefficient at a given concentration is $D_t = \Gamma/q^2$ where q is the scattering vector given by $4\pi n\lambda^{-1}\sin(\theta/2)$ where *n* is the water refractive index and θ is the scattering angle.

Turbidimetric and UV-vis measurements were performed with a Beckmann DU 650 spectrometer.
The ITC experiments were carried out at 298 K by means of a nano-ITC200 calorimeter (MicroCal). The amount of approximately 40 μL of quercetin solution (2 mmol dm^{-3}) was injected into the thermally equilibrated ITC cell (202 μL) filled with the CD solution (0.1 mmol dm^{-3}). The solvent was phosphate buffer (pH=6.9)/MeOH 6:4. The heat effect was measured after each addition of 2 μL and corrected by dilution effects.
The dispersions were sonicated with an ultrasound bath VWR Ultrasonic Cleaner (power 200 W, frequency 75 MHz).
ζ-potential measurements were performed by means of a ZETASIZER NANO ZS90 (Malvern Instruments).
Steady-state fluorescence spectra were acquired with a JASCO FP-777W spectrofluorimeter. Excitation and emission slits were 1.5 and 3 nm, respectively, excitation wavelength was 372 nm and emission interval was between 300 and 750 nm.

Synthesis of heptakis-6-(tert-butyldimethylsilyl)-2-propaneoxy-2-hexanethio-β-cyclodextrin

In a quartz test tube the heptakis-6-(tert-butyldimethylsilyl)-2-allyloxy-β-cyclodextrin[29] (100 mg, 46.2 mmol, 1eq) and the hexanethiol (0.23 mL, 1.62 mmol, 35eq) were dissolved, in distilled 95 % toluene/MeOH (concentration of CD was 5mM). A stream of Ar was bubbled through the solution for 15 min to thoroughly degas it. The test tube, kept under an atmosphere of Ar, was placed in front of a Hg lamp (265 nm) and stirred for 20 h. Following removal of solvent, the residue was washed three times with hexane and purified by chromatography (SiO_2, from 100 % hexane/EtOAc to 50 % hexane/EtOAc) to afford the product as a white solid (yield 82 %).
^{1}H NMR (DMSO, 300 K, 300 MHz) δ: 0.2 (42H, s), 0.88 (21H, t, J=9.5 Hz), 0.98 (63H, s), 1.30 (28H, m), 1.42 (14H, m), 1.63 (14H, m), 1.90 (14H, m), 2.68 (14H, m), 2.79 (14H, m), 3.37(14H, t, J=7.4 Hz), 3.02 (7H, dd, J=3.0 Hz, J=9.5 Hz), 3.54 (14H, m), 3.59 (7H, bs), 3.79 (7H, m), 3.99 (14H, m), 4.94 (7H, d, J=3.3 Hz).
^{13}C NMR (DMSO, 300 K, 75 MHz) δ: 4.9, 14.1, 22.7, 25.9, 28.2, 30.6, 30.8, 31.1, 33.2, 73.5, 62.5, 74.4, 74.9, 75.9, 79.7, 102.0.

Synthesis of compounds 3a-d

The appropriate thiol **2a-d** (1000 eq) and modified HNT **1** (100 mg) were dissolved in anhydrous toluene. A stream of Ar was bubbled through the solution for 15 min to thoroughly degas it. The solution, kept under an atmosphere of Ar, was placed in front of a Hg lamp and stirred for 24 h. Following removal of solvent, the precipitate was washed with CH_2Cl_2 and dried overnight at 80 °C under vacuum.

General procedure to obtain 3a/biological molecule dispersions

Varying weighed amounts of p-HNT or **3a** (from 2 up to 14 mg) were dispersed by sonication for 5 minutes in H_2O, at an ultrasound power of 200 W and a temperature of 25 °C. 1 mL of appropriate biological molecule solution (1×10^{-4} M) in a mixture pH 6.9 buffer/EtOH (6:4) was added to the p-HNT or **3a** dispersions. The final volume was 10 mL.

General procedure to obtain solid complexes

To a dispersion of **3a** in deionized water (5 mL) 1 mL of silibinin solution 10^{-2} M in ethanol was added. The suspension was sonicated for 5 min, at an ultrasound power of 200 W and at 25 °C and then was evacuated for 3 cycles. The suspension was left under stirrer for 24 h at room temperature. After this time the powder was washed with water and then dried at 80 °C under vacuum. Afterwards **3a**/silibinin solid complex was suspended again in deionized water (5 mL) and 1 mL of quercetin solution (10^{-2} M) in ethanol was, then, added. The suspension was stirred for 4 days at r.t. and then was filtered, the powder was washed with small amounts of water and then dried at 70 °C under vacuum overnight.

General procedure for spectrophotometric measurements

Measurement solutions were prepared by adding increasing volumes of the solution of heptakis-6-(tert-butyldimethylsilyl)-2-propaneoxy-2-hexanethio-β-cyclodextrin in phosphate buffer (pH 6.9) ($1.2\cdot10^{-3}$ M) to 100 μL of the quercetin aqueous solution into a volumetric flask. In these solutions, the concentrations of the quercetin was constant and equal to $1\cdot10^{-5}$ M while the concentration of the heptakis-6-(tert-butyldimethylsilyl)-2-propaneoxy-2-hexanethio-β-cyclodextrin increased from $1.2\cdot10^{-4}$ M up to $1.08\cdot10^{-3}$ M. The absorbance was recorded at 370 nm and spectroscopic data were fitted by the following equation (the non-linearized version of Benesi–Hildebrand treatment):

$$CD + Que \xrightleftharpoons{K_1} CD - Que$$

$$CD - Que + CD \xrightleftharpoons{K_2} CD - Que - CD$$

$$\Delta A = \frac{\Delta\varepsilon \cdot \beta \cdot Que \cdot [CD]^2}{1 + \beta \cdot [CD]^2} \qquad \text{(eq. 1)}$$

$$\beta = K_1 \cdot K_2$$

where $\Delta\varepsilon$ is the difference of extinction molar coefficient of free and complexed quercetin, *Que* and *CD* are the total concentration of the quercetin and heptakis-6-(tert-butyldimethylsilyl)-2-propaneoxy-2-hexanethio-β-cyclodextrin, respectively.

Kinetic Release

The release of quercetin and silibinin from the **3a**/Sil/Que complexes was done as following: 25 mg of the sample were dispersed in 1 mL of dissolution medium and transferred into a dialysis membrane (Medicell International Ltd MWCO 12-14000 with diameter of 21.5 mm). Subsequently the membrane was put in a round bottom flask containing 10 mL of the release medium at 37 °C and stirred.
Two different media (0.1 M HCl and phosphate buffer pH 7.4, respectively) were considered in order to evaluate the influence of pH on the release behavior of the drug.
At fixed time, 1 mL of the release medium has been withdrawn and analyzed by UV-vis (at 250 and 290 nm for quercetin and silibinin, respectively). To keep constant the volume of the release medium 1 mL of fresh solution (0.1 M HCl, pH 7.4 buffer) has been used to replace the collected one.

The quercetin and silibinin concentrations in the solution were determined by UV-vis spectrophotometry using the Lambert-Beer law.
Total amounts of drug released (F_t) were calculated as follows:

$$F_t = V_m C_t + \sum_{i=0}^{t-1} V_a C_i \qquad \text{(eq. 2)}$$

where V_m and C_t are volume and concentration of the drug at time t. V_a is the volume of the sample withdrawn and C_i is drug concentration at time i ($i<t$).

Cell culture

8505c anaplastic thyroid cancer cells (ECAC Sigma-Aldrich, Milan, Italy) were grown in RPMI1640 (Sigma-Aldrich, Milan, Italy) supplemented with 10% FCS (Sigma-Aldrich, Milan, Italy), 2mM L-glutamine and penicillin-streptomycin and incubated at 37 °C in 5% CO2 and 100% humidity.

MTS assay

8505c cells were plated at 1500 cells per well in triplicate in a 96-well plate. After 24h of incubation, **3a**/Sil/Que drug suspension was added ranging from 100 µM to 0.391 µM. After 72 h of incubation the plate was washed with sterile PBS, to avoid colour interference from the **3a**/Sil/Que compound. 20µl of the CellTiter 96 AQueous One Solution (Promega, Milan, Italy) was added, and the plate incubated for 4 hours at 37°C. Absorbance at 490 nm was recorded with a plate reader (Multiskan™ TC Microplate Photometer, Thermo SCIENTIFIC, Milan Italy). Results were expressed as % of viability respect the control cells not treated.
IC_{50} was calculated using Global Optimization by Simulated Annealing Software (GOSA-fit) and was 27.6 µM ± 6.1 µM.

Fluorescence Microscopy

8505c cells were seeded in a Nunc Lab-Tek Chamber Slide (Nunc, Italy) at a density of 300,000 cells per slide in RPMI culture medium and incubated at standard conditions. After 24 hours **3a** was added at 10µM and incubated for 1 hours and 24 hours respectively. Slides were then extensively washed with PBS-containining Ca and Mg and counterstained with Evans Blue in PBS at 0.005%. Slides were observed with a Zeiss Axiophot fluorescence microscope with a FITC filter equipped with a Nikon DS-Fi1 CCD-camera.

Conclusions

We have developed a new nanocarrier composed of biodegradable halloysite nanotubes-amphiphilic cyclodextrin for the co-delivery of silibinin and quercetin as a potential combination therapy for the treatment of thyroid cancer.
Multicavity halloysite-nanotube materials were obtained by grafting amphiphilic cyclodextrin units onto the nanotube surface. The obtained materials were characterized by FT-IR spectroscopy, TGA and SEM investigations.
In order to exploit their ability as drug carrier we, also, performed turbidimetric analysis in aqueous medium, which showed that, depending on the alkyl chain length of alkyl groups on cyclodextrin, the materials were like aggregates. These results were confirmed by DLS and ζ-potential investigations.
We studied the binding abilities of the systems with two biological active molecules, namely quercetin and silibinin.
HPLC measurements and fluorescence spectroscopy highlighted that silibinin interacts preferentially with HNT lumen, while quercetin does with cyclodextrin cavity.
The kinetic release of the two molecules from the multicavity system was also carried out. In addition, TGA results showed that the new materials can load with efficiency the drugs and therefore, they are suitable nanocontainers for co-delivery of two drugs that could have synergic effects in anticancer therapy as demonstrated by in *vitro* cytotoxic assays.
Finally, the interaction between cells and the carrier, analyzed by fluorescence microscopy, revealed that the materials were uptaken into cells surrounding the nuclei. Therefore the multicavity systems could transport drugs into living cells.

Acknowledgements

The work was financially supported by the University of Palermo, PRIN 2010-2011 (prot. 2010329WPF) and FIRB 2012 (prot. RBFR12ETL5).

Notes and references

[a] *Dipartimento STEBICEF, Sez. Chimica, Università degli Studi di Palermo, Viale delle Scienze, Parco d'Orleans II, Ed. 17, 90128 Palermo, Italy. E-mail: serena.riela@unipa.it; Fax: +39-091596825; Tel: +39-09123897546.*

[b] *Dipartimento Biomedico di Medicina Interna e Specialistica, sez. Endocrinologia, Diabetologia, Metabolismo, Università degli Studi di Palermo, 90127 Palermo, Italy.*

[c] *Dipartimento di Fisica e Chimica, Universit`a degli Studi di Palermo, Viale delle Scienze, Parco d'Orleans II, Ed. 17, 90128 Palermo, Italy. E-mail: giuseppe.lazzara@unipa.it.*

Electronic Supplementary Information (ESI) available: FT-IR spectra, TGA details and details about p-HNT/silibinin and p-HNT/quercetin complexes. See DOI: 10.1039/b000000x/

1 Y. Lvov and E. Abdullayev, *Progr. Polym. Sci.*, 2013, **38**, 1690.
2 a) S. Riela, M. Massaro, C. G. Colletti, A. Bommarito, C. Giordano, S. Milioto, R. Noto, P. Poma and G. Lazzara, *Int. J. Pharm.*, 2014, **475**, 613; b) M. Massaro, C. G. Colletti, R. Noto, S. Riela, P. Poma, S. Guernelli, F. Parisi, S. Milioto and G. Lazzara, *Int. J. Pharm.*, 2015, **478**, 476; c) E. Joussein, S. Petit, J. Churchman, B. Theng, D. Righi and B. Delvaux, *Clay Miner.* 2005, **40**, 383.
3 V. Vergaro, Y. M. Lvov and S Leporatti, *Macromol. Biosci.*, 2012, **12**, 1265.
4 H. Kelly, P. Deasy, E. Ziaka and N. Claffey, *Int. J. Pharm.*, 2004, **274**, 167.
5 D. Kommireddy, I. Ichinose, Y. M. Lvov and D. Mills, *J. Biomed. Nanotechnol.*, 2005, **1**, 286.
6 Y. F. Shi, Z. Tian, Y. Zhang, H. B. Shen and N. Q. Jia, *Nanoscale Res. Lett.*, 2011, **6**, 608.
7 A. D. Hughes, J. Mattinson, J. D. Powderly, B. T. Greene and M. R. King, *J. Vis. Exp.*, 2012, **64**, 4248.
8 G. Soloperto, F. Conversano, A. Greco, E. Casciaro, E. Ragusa, A. Lay-Ekuakille and S. Casciaro, *IEEE T Instrum Meas.*, 2013, **63**, 1423.
9 P. Lo Meo, F. D'Anna, S. Riela, M. Gruttadauria and R. Noto, *Tetrahedron*, 2002, **58**, 6039.
10. L. Zerkoune, A. Angelova and S. Lesieur, *Nanomaterials* 2014, **4**, 741.

11. M. Massaro, S. Riela, P. Lo Meo, R. Noto, G. Cavallaro, S. Milioto and G. Lazzara, *J. Mater. Chem. B*, 2014, **2**, 7732.
12. W. Y. Huang, Y. Z. Cai and Y. Zhang, *Nutr. Cancer*, 2010, **62**, 1.
13. B. Buhklari, S. Memon, M. M. Tahir and M. I. Bhanjer, *J. Mol. Struct.*, 2008, **892**, 39.
14. Y. Wei, X. Ye, X. Shang, X. Peng, Q. Bao, M. Liu, M. Guo and F. Li, *Eng. Aspects*, 2012, **396**, 22.
15. Y. Zheng, I. S. Haworth, Z. Zuo, M. S. S. Chow and A. H. L. Chow, *J. Pharm. Sci.*, 2005, **94**, 1079.
16. A. Kumari, S. K. Yadav, Y. B. Pakade, B. Singh and S. C. Yadav, *Colloids Surf. B*, 2010, **80**, 184.
17. a) C. Poon, C. He, D. Liu, K. Lu and W. Lin, *J. Controll. Rel.* 2015, 10.1016/j.jconrel.2015.01.026; b) H. Wang, Y. Wu, R. Zhao and G. Nie, *Adv. Mater,* 2013, **25**, 1616; c) J. Lehar, A. S. Krueger, W. Avery, A. M. Heilbut, L. M. Johansen, E. R. Price, R. J. Rickles, G. F. Short, 3rd, J. E. Staunton, X. Jin, M. S. Lee, G. R. Zimmermann and A. A. Borisy, *Nat Biotechnol.,* 2009, **27**, 659.
18. P. Yuang, P. D. Southon, Z. Liu, M. E. R. Green, J. M. Hook, S. J. Antill and C. J. Kepert, *J. Phys. Chem. C*, 2008, **112**, 15742.
19. *Interfacial Phenomena: Equilibrium and Dynamic Effects*, C. A. Miller, P. Neogi, New York, Marcel Dekker, inc., 1985, vol. 17.
20. G. Cavallaro, G. Lazzara and S. Milioto, *Langmuir*, 2011, **27**, 1158.
21. F. Perret, C. Marminon, W. Zeinyeh, P. Nebois, A. Bollacke, J. Jose, H. Parrot-Lopez and M. Le-Borgne, *Int. J. Pharm.* 2013, **441**, 491.
22. C. Jullian, L. Moyano, C. Yañez, and C. Olea-Azar, *Spectrochim. Acta Part A*, 2007, **67**, 230.
23. R. De Lisi, G. Lazzara and S. Milioto, *Phys. Chem. Chem. Phys.*, 2011, **13**, 12571.
24. H. Liu, Z. Du and Q. Yuan, *J. Chrom. B*, 2009, **877**, 4159.
25. K. M. Tushar, S. G. Kalyan, S. Anirban and D. Swagata, *J. Photochem. Photobiol. A: Chem.*, 2008, **194**, 297.
26. R. Angelico, A. Ceglie, P. Sacco, G. Colafemmina, M. Ripoli and A. Mangia, *Int. J. Pharm.*, 2014, 471, 173.
27. X. Zhu and W. Ping, *Spectrochim. Acta Part A: Mol. Biomol. Spectr.*, 2014, **132**, 38.
28. I. Calabrese, G. Cavallaro, C. Scialabba, M. Licciardi, M. Merli, L. Sciascia and M. L. Turco Liveri, *Int. J. Pharm.*, 2013, **457**, 224.
D. A. Fulto, and J. F. Stoddart, *J. Org. Chem.* 2001, **66**, 8309.

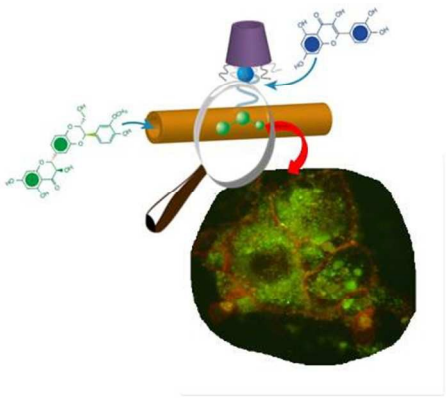

254x190mm (96 x 96 DPI)